Paddy rice traits estimation under varying management strategies using UAV technology

Daniel Muhindo, Joyce J Lelei, Wivine Munyahali, Landry Cizungu, Sebastian Doetterl, Florian Wilken, Espoir Bagula, Nathan Okole, Boris Rewald, Samuel Mwonga

▶ **To cite this version:**

Daniel Muhindo, Joyce J Lelei, Wivine Munyahali, Landry Cizungu, Sebastian Doetterl, et al.. Paddy rice traits estimation under varying management strategies using UAV technology. Agrosystems, Geosciences & Environment, 2025, 8 (1), pp.e70047. ⟨10.1002/agg2.70047⟩. ⟨hal-04947435⟩

HAL Id: hal-04947435

https://hal.science/hal-04947435v1

Submitted on 14 Feb 2025

HAL is a multi-disciplinary open access archive for the deposit and dissemination of scientific research documents, whether they are published or not. The documents may come from teaching and research institutions in France or abroad, or from public or private research centers.

L'archive ouverte pluridisciplinaire **HAL**, est destinée au dépôt et à la diffusion de documents scientifiques de niveau recherche, publiés ou non, émanant des établissements d'enseignement et de recherche français ou étrangers, des laboratoires publics ou privés.

Distributed under a Creative Commons CC BY-NC-ND 4.0 - Attribution - Non-commercial use - No Derivative Works - International License

Check for updates

Received: 15 April 2024 | Accepted: 5 January 2025

DOI: 10.1002/agg2.70047

Agrosystems, Geosciences & Environment OPEN ACCESS

ORIGINAL ARTICLE

Special Section: Enhancing Food Security through Innovative Agricultural Management

Paddy rice traits estimation under varying management strategies using UAV technology

Daniel Muhindo[1,2,3] | **Joyce J. Lelei**[2] | **Wivine Munyahali**[1,3] | **Landry Cizungu**[1] | **Sebastian Doetterl**[4] | **Florian Wilken**[5] | **Espoir Bagula**[6] | **Nathan Okole**[6,7] | **Boris Rewald**[8,9] | **Samuel Mwonga**[2]

[1]Faculty of Agronomy, Université Catholique de Bukavu (UCB), Bukavu, Democratic Republic of the Congo

[2]Department of Crops Horticulture and Soils, Egerton University, Nakuru, Kenya

[3]Departement agrovétérinaire, Institut Supérieur des Techniques de Développement de Kalehe, Kalehe, Democratic Republic of the Congo

[4]Department of Environmental Systems Science, Eidgenössische Technische Hochschule Zürich, Zürich, Switzerland

[5]Institute for Geography, Universität Augsburg, Augsburg, Germany

[6]Faculty of Agronomy, Université Evangélique en Afrique, Bukavu, Democratic Republic of the Congo

[7]Institute of Sugar Beet Research, Göttingen, Germany

[8]University for Natural Resources and Life Sciences Vienna, Vienna, Austria

[9]Faculty of Forestry and Wood Technology, Department of Forest Protection and Wildlife Management (FFWT), Mendel University in Brno, Brno, Czech Republic

Correspondence
Daniel Muhindo, Faculty of Agronomy, Université Catholique de Bukavu (UCB), P.O. Box 285 Bukavu, Democratic Republic of the Congo.
Email: muhindo.iragi@ucbukavu.ac.cd

Assigned to Associate Editor Kirsten Verburg.

Boris Rewald and Samuel Mwonga are joint senior authors.

Abstract

Timely crop monitoring and yield prediction are essential in guiding management decision making. The aim of the study was to estimate the agronomic traits of paddy rice (*Oryza sativa* L.) using unmanned aerial vehicle (UAV)-multispectral imaging. A randomized complete block design field experiment with a split–split plot arrangement was set up in the Ruzizi plain, Democratic Republic of Congo (DRC). Spectral imaging data were collected at rice tillering and panicle initiation stages. Predictive analysis of rice agronomic traits was performed using linear and decision tree-based machine learning techniques. Paddy rice trait predictions were critically sensitive to the timing of image acquisition but not largely affected by the model. The most accurate predictions were made at rice panicle initiation stage, with R^2 values of 0.62, 0.65, and 0.75 for yield, aboveground biomass, and plant nitrogen (N) uptake, respectively. The visible atmospherically resistant index (VARI), modified chlorophyll absorption in reflective index, and ratio vegetation index, along with near

Abbreviations: AGB, aboveground biomass; AWD, alternate wetting and drying; BC, biochar; DAT, days after transplanting; DRC, Democratic Republic of Congo; ERT, extremely randomized trees; MCBC, manure-charged biochar; MLR, multiple linear regression; PF, permanent flooding; PNU, plant nitrogen uptake; RF, random forest; SVM, support vector machine; UAV, unmanned aerial vehicle.

This is an open access article under the terms of the Creative Commons Attribution-NonCommercial-NoDerivs License, which permits use and distribution in any medium, provided the original work is properly cited, the use is non-commercial and no modifications or adaptations are made.
© 2025 The Author(s). *Agrosystems, Geosciences & Environment* published by Wiley Periodicals LLC on behalf of Crop Science Society of America and American Society of Agronomy.

infrared and green bands, played a critical role in predicting paddy rice N uptake and yield. The same spectral features associated with crop height and canopy data were essential for predicting paddy rice aboveground biomass. UAV-multispectral data were able to assess agricultural intensification strategies at field/landscape scale irrespective of soil types, watering regimes, and cultivars. Special consideration should be attributed to VARI, as it enables economical prediction of paddy rice traits. The UAV technologies are therefore reliable tools for monitoring rice production and can be applied in agricultural extension in the DRC.

1 | INTRODUCTION

Rice (*Oryza sativa* L.) is the second most important cereal crop in the Democratic Republic of Congo (DRC), after maize (*Zea mays* L.) (Bulambo et al., 2023). The Ruzizi plain, a vast lowland area in South Kivu province covering 80,000 ha, is one of the most important rice-producing regions in the country (Walangululu et al., 2012). The production, however, does not meet local demand, potentially due to poor soil and water management practices carried out by farmers (Vwima & Rushigira, 2020). For example, most farmers apply fertilizer at low or suboptimal rates due to high costs (Balasubramanian et al., 2007; Suvi et al., 2020). In addition, most rice fields are flooded, which greatly reduces the efficiency with which nutrients, particularly nitrogen (N), are used by the crop (Mboyerwa et al., 2022).

Crop monitoring is therefore needed to support management decisions such as fertilizer application and to close the rice yield gap. This is particularly crucial at the vegetative phase—specifically at tillering and panicle initiation stages, during which N fertilizer top dressing is commonly done by rice farmers in the Ruzizi plain (Walangululu et al., 2012)—in order to provide timely information about the spatial distribution of plant nitrogen uptake (PNU) or growth/vigor in the field and design feasible N fertilizer application strategies (L. Wang et al., 2021). Traditional crop diagnostic methods involve destructive biomass sampling and laboratory analysis. These methods are costly, labor-intensive, and time-consuming, making them less suitable for timely and site-specific management decisions (Osco et al., 2020; Peng et al., 2022). Remote sensing technology, however, has the potential to non-destructively assess important plant agronomic traits such as aboveground biomass (AGB), yield, and N status with high spatial precision and at variable scales (Lussem et al., 2022).

While remotely sensed images were initially acquired via satellites and aircraft (Hassler & Baysal-Gurel, 2019), either with low spatiotemporal resolution or at great expense (X. Li et al., 2022), remote sensing by unmanned aerial vehicles (UAVs) has developed over the last decade into a rapid, real-time, high-resolution, and non-destructive means of field monitoring (Peng et al., 2022). When equipped with multi- or hyperspectral sensor systems, or by reconstructing spectral patterns from Red-Green-Blue (RGB) images, UAV technology is thus a promising approach for monitoring crop growth status and nutrient content, as well as yield prediction (Osco et al., 2020; Zhao et al., 2022). Concurrent advances in data processing software allow for increasingly automated development of image products (Zha et al., 2020). In particular, machine learning (ML) methods can discover hidden information in data, making them popular in complex and data-intensive fields, such as remote sensing and precision agriculture (Lussem et al., 2022; Qiu et al., 2016). While many researchers have achieved satisfactory predictions of agronomic traits using ML models (Liu et al., 2023; L. Wang et al., 2021), the accuracy of the models used varies depending on the geographical location and the timing of imaging along the cropping cycle (Han et al., 2020; Rehman et al., 2022). Furthermore, as the importance of predicting features varies depending on the subject being investigated, it is common practice to evaluate different approaches or combinations of input data when working with agricultural remote sensing (Weiss et al., 2020).

Despite its potential, studies on the use of UAV in agriculture and the application of ML to UAV-collected data are still limited in Sub-Saharan Africa. In addition, because it is difficult to propose universal models or general methods for retrieving crop phenotypic traits that allow for high accuracy crop monitoring using UAV-based remote sensing, field and region-based phenotyping studies using UAV-based remote sensing remain necessary. However, to our knowledge, no study has investigated the potential of UAV imaging and ML techniques to predict paddy traits under contrasting irrigation regimes (alternate wetting and drying [AWD] vs. continuous flood irrigation), different nutrient management practices (no fertilization, mineral fertilizer (NPK), combined biochar [BC], and fertilizer application), and different varieties, in order to develop sensor-based recommendations that can improve rice production in eastern DRC. The suggested nutrient and water management practices are crucial

26396696, 2025, 1, Downloaded from https://acsess.onlinelibrary.wiley.com/doi/10.1002/agg2.70047 by CochraneAustria, Wiley Online Library on [14/02/2025]. See the Terms and Conditions (https://onlinelibrary.wiley.com/terms-and-conditions) on Wiley Online Library for rules of use; OA articles are governed by the applicable Creative Commons License

in the rice-producing areas of the Ruzizi plain region, which is known for its Phaeozems soils with low nutrient levels (Birindwa et al., 2023) and where water availability is no longer permanently assured due to extended dry seasons caused by climate variability (Espoir et al., 2021). Studies have shown that the combined application of BC and NPKs can improve the nutrient use efficiency, especially N, in rice-based systems (MacCarthy et al., 2020; Oladele et al., 2019). Additionally, implementing AWD irrigation techniques can reduce overall water consumption while still providing the necessary amount of water to the rice crop during crucial growth stages, thus avoiding any negative effects on yield and grain quality (Ramos-Fernández et al., 2024).

Therefore, the research questions associated to this study were as follows: (1) What is the most effective timing for UAV-spectral imaging during the rice vegetative phase to estimate AGB and PNU, as well as to predict the yield of rice in the Ruzizi plain? (2) What ML models and UAV-imaging features provide the most accurate estimation/prediction for rice traits in the Ruzizi plain? (3) Can UAV-multispectral imaging features effectively differentiate paddy rice fields managed with varying levels of water and nutrient availability?

The objectives of this study were: (1) assess the most effective time at vegetative phase for estimating AGB and PNU and predicting yield of rice in the Ruzizi plain, Eastern DRC, using UAV-spectral imaging data and ML techniques; (2) determine the most relevant spectral and structural features and models for paddy rice trait estimations/predictions; and (3) evaluate the potential of the features in detecting differences in management practices varying in water and nutrient availabilities.

Core Ideas

- Unmanned aerial vehicle (UAV)-multispectral data were able to assess agricultural intensification strategies at field/landscape scale.
- Rice trait predictions were critically sensitive to the timing of image acquisition but not largely affected by the model.
- More accurate predictions were obtained at rice panicle initiation stage than at the tillering stage.
- The UAV technologies are reliable tools for monitoring paddy rice production and can be applied in agricultural extension in the Democratic Republic of Congo.

2 | MATERIALS AND METHODS

2.1 | Study sites

Field experiments were replicated at two rice-producing sites, namely, Kiringye (2.895° S, 28.999° E, 904 m a.s.l), and Lubarika (2.818° S, 28.963° E, 910 m a.s.l.) in the Ruzizi plain, South Kivu province, DRC (Figure 1). The experiments were carried out between February and May 2022. Both Kiringye and Lubarika soils have a loamy sand texture and bulk densities of 1.45 g cm^{-3} and 1.32 g cm^{-3} at a depth of 0–20 cm, respectively. The pH values recorded at the Lubarika and Kiringye sites were similar, with values of 6.41 and 6.61, respectively. However, the Kiringye soils had higher average concentrations of total organic carbon (2.2%), total N (0.11%), available phosphorus (30.12 mg kg^{-1}), and cation exchange capacity (26.3 cmol kg^{-1}) than the Lubarika soils (0.95%, 0.1%, 26.3 mg kg^{-1}, and 13 cmol kg^{-1}, respectively; Table S1). The cumulative precipitation recorded during the four-month experimental period was 339 mm in Lubarika and 410 mm in Kiringye. The mean temperatures observed during this period were 24.9°C and 25.1°C in Kiringye and Lubarika, respectively.

2.2 | UAV image acquisition and pre-processing

Data collection took place at the active tillering (30 days after transplanting [DAT]) and panicle initiation (60 DAT) stages of rice. Flights were performed with a Phantom 3 professional UAV (DJI) equipped with a multispectral camera (RedEdge-M; Micasense). The camera has five spectral bands: blue (475 nm), green (560 nm), red (668 nm), red-edge (717 nm), and near infrared (NIR) (840 nm). The altitude of the UAV flights was set at 15 m above the ground and the speed at 1 m s^{-1} to ensure both high spatial resolution and image overlap. The obtained ground sampling distance averaged 1.25 cm $pixel^{-1}$. Prior to each flight, the camera was calibrated using a grey plate with reflectance values of 0.62, 0.63, 0.62, 0.62, and 0.58 for blue, green, red, red-edge, and NIR bands, respectively. The UAV missions were conducted between 10:00 a.m. and 03:00 p.m. (local time) under windless and clear-sky conditions. The two experimental sites were imaged on two consecutive days.

Autopilot software was used for mission control and image acquisition. After data acquisition, the Pix4d Mapper software (version 4.3.31; Pix4d S.A.) was used to combine the images and generate the mosaic images, digital elevation model (DEM), digital surface model (DSM), and reflectance maps of the experimental areas. During this process, five to six ground control points, taken with a real-time kinematic global navigation satellite system (RTK GNSS) (Reach RS+; EMLID), were used to orthorectify and georeference the mosaic. A total of five UAV reflectance orthoimages per

26396696, 2025, 1, Downloaded from https://acsess.onlinelibrary.wiley.com/doi/10.1002/agg2.70047 by CochraneAustria, Wiley Online Library on [14/02/2025]. See the Terms and Conditions (https://onlinelibrary.wiley.com/terms-and-conditions) on Wiley Online Library for rules of use; OA articles are governed by the applicable Creative Commons License

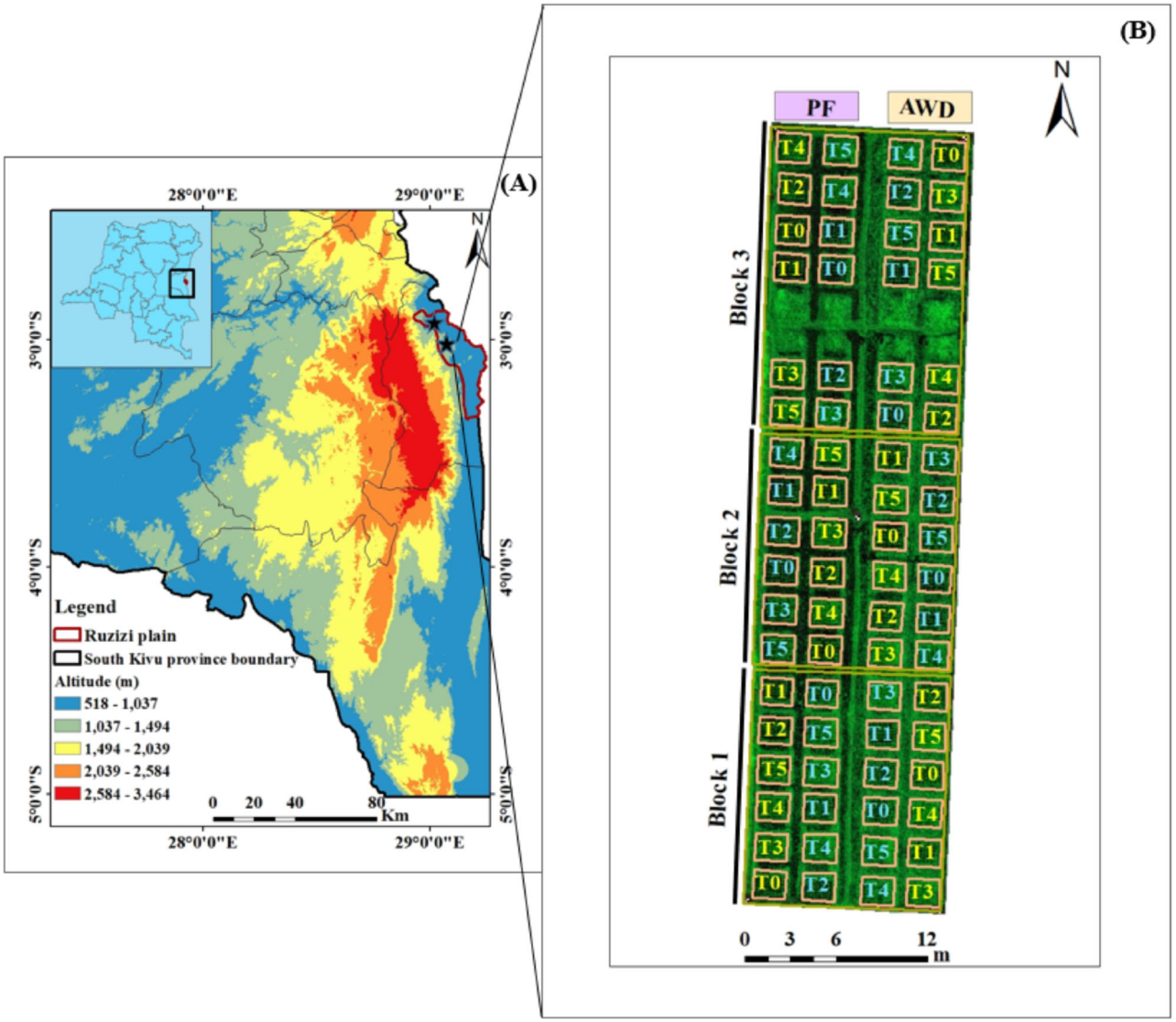

FIGURE 1 (A) Ruzizi plain, South Kivu province, Democratic Republic of Congo (DRC); Kiringye and Lubarika experimental sites are marked with black stars. (B) Experimental design at the Kiringye site. Treatments: T0: Unfertilized control, T1: Biochar (BC), T2: Manure-charged biochar (MCBC), T3: mineral fertilizer (NPK), T4: NPK + BC, T5: NPK + MCBC. AWD: alternate wetting and drying; PF, permanent flooding irrigation. Yellow: TAI cultivar, Blue: AR2017105 cultivar; see text for details.

crop stage were obtained for each site. The plot boundaries were digitized and used as regions of interest for selecting and averaging reflectance values to relate to ground truth data.

2.3 | Experimental set-up

The rice cultivars used in the study were TAI and AR2017105. The cultivar TAI is commonly used by farmers in the Ruzizi plain and the cultivar AR2017105 is a new cultivar introduced in 2021 by the provincial ministry of agriculture in the Ruzizi plain (Table S2) (IPA, 2021; IRRI, 2012). Both cultivars have a cropping cycle of about 120 days. TAI cultivar is 63.5% taller, has longer panicles and fewer tillers (12) than AR2017105 cultivar (15 tillers). Seeds were derived from the provincial Ministry of Agriculture. Their germination was done in a seedbed. Fifty-six similar sized rice seedlings were planted in each plot, 14 days after germination. To create a large range of agronomic conditions, mimicking potential management effects on N and water availability, we set up experiments at both sites (Figure 1B). A randomized complete block design with a split–split plot arrangement, and three replications was used. The main plots consisted of two water management schemes: AWD cycles or permanent flooding (PF). The subplots were cultivars (TAI and AR2017105) and fertilization, the sub-subplots. Water was applied continuously throughout the season in PF plots. AWD plots were

26396696, 2025, 1, Downloaded from https://acsess.onlinelibrary.wiley.com/doi/10.1002/agg2.70047 by CochraneAustria, Wiley Online Library on [14/02/2025]. See the Terms and Conditions (https://onlinelibrary.wiley.com/terms-and-conditions) on Wiley Online Library for rules of use; OA articles are governed by the applicable Creative Commons License

reflooded when the water level dropped to 15 cm below the soil surface (Mote & Velchala, 2021). During panicle initiation and flowering, AWD plots were kept flooded for 4 weeks. Perforated tubes were installed in the center of all AWD plots to monitor water levels (Mote & Velchala, 2021). Fertilization levels consisted of unfertilized control (Ctrl; T0), rice husk BC (T1), manure-charged biochar (MCBC; T2), NPK (T3), NPK + BC (T4), and NPK + MCBC (T5).

The two types of (BC and MCBC) were applied at a rate of 5 t ha^{-1} and NPK was applied at a rate of 102 kg N ha^{-1}, 25 kg P_2O_5 ha^{-1} and 51 kg K_2O ha^{-1}. BC production procedures, characteristics and nutrient content are given in Supporting Information S1, Table S3. Full rates of BC were uniformly spread over the plots and then incorporated into the soil to a depth of 20 cm 2 weeks before transplanting. NPKs were applied after seedling transplanting. Half of the urea was applied at the time of transplanting (0 DAT; day after transplanting), 25% at active tillering (30 DAT) and 25% at panicle initiation (60 DAT). Phosphorus and potassium were applied as triple superphosphate and muriate of potash, respectively at full rates during transplanting. The fertilization treatments are considered to create a gradient of N availability, from the least N availability hypothesized under control conditions (T0) to excess plant N availability in the treatment combining mineral fertilization with MCBC (NPK + MCBC; T5).

To control water movement and to minimize nutrient leaching from neighboring plots, 30 cm high and 30 cm wide dikes were built around each plot at each experimental site. In total, 72 experimental plots were established at each site. The size of each plot was 2.8 m^2 (1.4 m × 2 m).

2.4 | Field data collection and plant nitrogen content analysis

After spectral data collection, three plant samples consisting of stems, leaves and on-setting grains, were randomly selected from each plot and excised at the base for AGB measurement (Yu et al., 2013). The sampled plants from each plot were mixed, brush-cleaned, chopped and oven-dried at 70°C for 48 h, and then weighed to an accuracy of ± 0.1 mg. The samples were thereafter ground for measurement of plant nitrogen concentration (PNC). Analysis of PNC was done using a LECO-CN analyzer (Leco Corp.), at laboratories of the University of Natural Resources and Life Sciences, Vienna, Austria. PNU was calculated by multiplying PNC by AGB (Zha et al., 2021). Grain yield was measured at rice physiological maturity (120 DAT) from 30 plants in each plot, excluding border plants. The yield was determined at 1.3 g kg^{-1} grain moisture content, measured using a digital moisture meter (LDS-1G grain moisture meter, SKZ industrial).

2.5 | Data analysis

2.5.1 | Model and input data approaches

Four different modeling strategies were compared. These were two linear-based models [multiple linear regression (MLR) and support vector machine (SVM)] and two decision tree-based models (random forest [RF] and extremely randomized trees [ERT]) (Geurts et al., 2006; Peng et al., 2022; Uyanık & Güler, 2013). To build empirical models for predicting yield, biomass, and N uptake, the input data used were raw reflectance data, vegetation indices (VIs), and crop features, including the height and canopy cover. VIs were computed using all five bands of the multispectral camera. A total of 10 VIs were selected, which are detailed in Table S4. These included the normalized difference vegetation index (NDVI), the normalized difference red-edge index (NDRE), green NDVI (GNDVI), chlorophyll index-red-edge (CIRE), blue NDVI, ratio vegetation index (RVI), optimized soil adjusted vegetation index, green red vegetation index, modified chlorophyll absorption in reflective index (MCARI), and visible atmospherically resistant index (VARI) (Brewer et al., 2022; Dimyati et al., 2023; Stavrakoudis et al., 2019).

The canopy cover and height features were generated from DEM and DSM obtained after image pre-processing in Pix4d software (Yang et al., 2017). The crop height was generated as the difference between DSM and DEM, while the crop cover was obtained by threshold-based image segmentation using the NDVI combined with Otsu's automatic thresholding method (Xu et al., 2011). This method helped to find the optimal threshold separating vegetation (rice), soil, and water regions with maximum interclass variance. Crop cover within a plot was calculated as the percentage of pixels classified as vegetation within that plot (1.25 cm × 1.25 cm spatial resolution). All the spectral and crop features were extracted and aggregated at plot level to make up the final dataset with 72 entries for each site.

In this study, four approaches to input data combination were tested to assess the sensitivity and minimum input requirements for robust plant trait prediction: (i) use of spectral bands alone, (ii) VIs alone, (iii) combined spectral bands with VIs, and (iv) other crop-related features such as the DSM-derived crop cover and height.

To ensure the robustness of the trained model, multicollinearity within the input data were addressed by recursively eliminating features using the variance inflation factor (VIF). In this study, a VIF cut-off value of 20 (O'Brien, 2007) was set for the iterative removal of multicollinear features. At each iteration, the feature with the highest VIF value was removed until no feature had a VIF >20. This approach ensured that the best set of variables (i.e., with minimal collinearity) was retained for further processing.

26396696, 2025, 1, Downloaded from https://acsess.onlinelibrary.wiley.com/doi/10.1002/agg2.70047 by CochraneAustria, Wiley Online Library on [14/02/2025]. See the Terms and Conditions (https://onlinelibrary.wiley.com/terms-and-conditions) on Wiley Online Library for rules of use; OA articles are governed by the applicable Creative Commons License

After feature selection, the selected features were used for model training. For the SVM, RF, and ERT models, the hyperparameters were optimized prior to model training using a randomized grid search approach using the Python ML library scikit-learn. For the SVM model, different *C*-values and kernels were included in the grid, and in the case of the radial basis function kernel, different gamma values were also included in the grid for testing. For the RF and ERT models, the optimized hyperparameters included the criterion, the number of trees in the forest, and the minimum number of samples per leaf. It is worth noting that this entire process was performed on the training set only, while the test set remained completely unseen throughout the training process, following a repeated stratified *k*-fold cross-validation approach as described in the "model evaluation section."

2.5.2 | Model evaluation

The performance of each model was assessed using the R^2 score, the root mean square error (RMSE) score, and the root mean square percentage error (RMSPE) score. All three scores were calculated on the left-apart fold, following a repeated stratified 10-fold cross-validation strategy with three repeats (Vanwinckelen & Blockeel, 2012). This is equivalent to performing a 90%–10% train-test split 30 times, that is, dividing our 72-plot sample size into 64–65 samples for training the model and 7–8 samples for testing the model. The stratification ensured that the training and testing datasets had equal proportions of low, medium, and high values of the target variable. Following this approach, each model was evaluated 30 times on unseen data, and the mean and standard deviation across the 30 evaluations were reported. It is worth noting that each model evaluation internally implemented a standard scaler to ensure that all input features had a zero mean and unit variance. The models with the highest R^2 and lowest RMSE and RMSPE were selected as the best models.

After model evaluation, the best model for each target variable and for each flight was retained to compute feature importance. For decision tree-based methods, feature importance was obtained by a permutation-based approach, which involved shuffling a single feature's values and measuring the resulting decrease in the model score (Hapfelmeier & Ulm, 2013). For linear-based estimators, feature importance was assessed by the absolute value of the respective coefficient after standardizing the features to have unit variance. In both cases, feature importance was transformed into percentages to ensure that they summed up to 100. Seven variables, including blue and red bands, GNDVI, CIRE, and MCARI, and height and canopy cover features were retained at the tillering stage, while eight variables, including reflectance at blue, green, and NIR bands, RVI, MCARI, and VARI indices, and height and canopy cover features, were selected at panicle initiation stage.

The best combination (model + input feature) for a given parameter was also used to generate observed versus predicted plots for each site. The dataset was stratified into three folds (Vanwinckelen & Blockeel, 2012), and the predictions for each fold were obtained from a model trained on the remaining twofolds. Finally, the N distribution maps were generated based on the predicted PNU using the model, which demonstrated the highest R^2 and lowest RMSE and RMSPE. Due to the higher accuracy of paddy rice trait predictions during the panicle initiation stage, attention was solely drawn to the feature importance and prediction maps from this stage in the results section.

2.5.3 | Statistical analysis

Python 3.9 was used to compute R^2, RMSE, and RMSPE for model evaluation, determine feature importance, generate predicted versus observed graphs, create correlation matrices between response variables and prediction features, and generate the N uptake distribution maps (Adão et al., 2017). Concerning the correlation analysis, an *r* absolute value of 0–0.19 was regarded as very weak, 0.2–0.39 as weak, 0.40–0.59 as moderate, 0.6–0.79 as strong, and 0.8–1 as a very strong correlation. To analyze the effect of watering regimes, cultivar, and fertilization on spectral indices, a three-way analysis of variance was performed using the R software package version 4.3.3 and R-studio (Espoir et al., 2021). Each time an effect was significant at the $p < 0.05$ level, the honestly significant difference the Tukey test was used for post hoc analysis. R software was also used to calculate the AGB, the PNU, and the yield descriptive statistics, including the means, the standard errors, and the coefficients of variation.

3 | RESULTS

3.1 | Measured PNU, AGB, and yield

Nitrogen uptake by rice in Lubarika and Kiringye varied from 108.30 to 242.95 kg N ha^{-1} and 57.70 to 154.14 kg N ha^{-1} at the tillering stage, and from 218.98 to 444.54 kg N ha^{-1} and 142.55 to 259.09 kg N ha^{-1} at the panicle initiation stage, respectively. AGB ranged from 4.14 to 7.33 Mg ha^{-1} and 3.11 to 6.90 Mg ha^{-1} at the tillering stage, and from 8.13 to 13.43 Mg ha^{-1} and 7.93 to 12.48 Mg ha^{-1} at the panicle initiation stage at Lubarika and Kiringye, respectively. Rice grain yield at physiological maturity varied from 4.77 to 8.46 Mg ha^{-1} in Lubarika and from 4.31 to 7.72 Mg ha^{-1} in Kiringye. At both sites, the highest PNU, AGB, and yield were observed in plots treated with NPK fertilizer, either alone or in

26396696, 2025, 1, Downloaded from https://acsess.onlinelibrary.wiley.com/doi/10.1002/agg2.70047 by CochraneAustria, Wiley Online Library on [14/02/2025]. See the Terms and Conditions (https://onlinelibrary.wiley.com/terms-and-conditions) on Wiley Online Library for rules of use; OA articles are governed by the applicable Creative Commons License

TABLE 1 Measured (means ± SE) aboveground biomass (AGB), plant nitrogen uptake (PNU), and yield of rice at the tillering stage and the panicle initiation stage at Ruzizi plains, Democratic Republic of Congo (DRC), field sites Lubarika and Kiringye, respectively.

		Lubarika			Kiringye		
		AGB (Mg ha^{-1})	PNU (kg N ha^{-1})	Yield (Mg ha^{-1})	AGB (Mg ha^{-1})	PNU (kg N ha^{-1})	Yield (Mg ha^{-1})
Tillering stage (30 DAT)							
Fertilization types	Control	4.14 ± 0.36	112.26 ± 12.25	4.97 ± 0.39	3.11 ± 0.30	57.81 ± 8.61	4.31 ± 0.31
	BC	4.34 ± 0.44	108.30 ± 11.01	4.77 ± 0.49	3.21 ± 0.35	57.70 ± 7.01	4.52 ± 0.25
	MCBC	4.18 ± 0.46	117.85 ± 16.60	4.99 ± 0.38	3.35 ± 0.37	64.98 ± 7.86	4.75 ± 0.21
	NPK	6.88 ± 0.57	221.45 ± 20.08	7.20 ± 0.35	6.25 ± 0.42	128.33 ± 9.24	6.84 ± 0.35
	NPK + BC	7.33 ± 0.43	242.95 ± 17.98	8.46 ± 0.55	6.90 ± 0.38	154.14 ± 11.05	7.16 ± 0.29
	NPK + MCBC	7.22 ± 0.33	240.56 ± 18.20	8.10 ± 0.39	6.65 ± 0.61	140.02 ± 16.15	7.72 ± 0.24
Cultivars	*AR2017105*	5.17 ± 0.36	157.73 ± 13.85	6.89 ± 0.36	4.08 ± 0.35	81.90 ± 7.90	6.21 ± 0.29
	TAI	6.19 ± 0.31	190.06 ± 13.30	5.94 ± 0.33	5.74 ± 0.35	119.09 ± 9.09	5.55 ± 0.27
Watering regimes	AWD	5.76 ± 0.38	185.75 ± 15.09	6.65 ± 0.34	5.27 ± 0.39	107.93 ± 9.51	5.73 ± 0.25
	PF	5.60 ± 0.32	162.05 ± 12.19	6.19 ± 0.37	4.55 ± 0.36	93.06 ± 8.44	6.04 ± 0.31
Panicle initiation stage (60 DAT)							
Fertilization types	Control	8.13 ± 0.56	218.98 ± 19.06	4.97 ± 0.39	7.93 ± 0.62	147.19 ± 12.8	4.31 ± 0.31
	BC	8.82 ± 0.77	221.07 ± 20.01	4.77 ± 0.49	8.00 ± 0.49	142.55 ± 11.30	4.52 ± 0.25
	MCBC	8.75 ± 0.74	243.73 ± 27.61	4.99 ± 0.38	8.45 ± 0.46	163.75 ± 12.56	4.75 ± 0.21
	NPK	12.74 ± 0.65	407.90 ± 22.48	7.20 ± 0.35	11.52 ± 0.41	236.42 ± 10.52	6.84 ± 0.35
	NPK + BC	13.36 ± 0.53	440.56 ± 25.42	8.46 ± 0.55	12.40 ± 0.43	277.26 ± 16.41	7.16 ± 0.29
	NPK + MCBC	13.43 ± 0.39	444.54 ± 24.24	8.10 ± 0.39	12.48 ± 0.58	259.09 ± 18.01	7.72 ± 0.24
Cultivars	*AR2017105*	10.21 ± 0.57	307.40 ± 21.78	6.89 ± 0.36	9.28 ± 0.47	183.73 ± 11.70	6.21 ± 0.29
	TAI	11.53 ± 0.45	351.52 ± 20.98	5.94 ± 0.33	10.98 ± 0.37	225.03 ± 11.48	5.55 ± 0.27
Watering regimes	AWD	10.68 ± 0.53	341.97 ± 22.86	6.65 ± 0.34	10.86 ± 0.44	219.64 ± 12.87	5.73 ± 0.25
	PF	11.06 ± 0.51	316.96 ± 20.27	6.19 ± 0.37	9.40 ± 0.41	189.11 ± 10.68	6.04 ± 0.31

Note: Six fertilization types, two rice cultivars, and two watering regimes were accessed.

Abbreviations: AWD, alternate wetting and drying; BC, biochar; Control, unfertilized control; DAT, days after transplanting; MCBC, manure-charged biochar; NPK + BC, mineral fertilizer + biochar; NPK + MCBC, mineral fertilizer + manure-charged biochar; NPK, mineral fertilizer; PF, permanent flooding; SE, standard error.

combination with BC, compared to plots treated with BC alone or left unfertilized. Additionally, the PNU and AGB were generally higher under AWD compared to PF, with TAI cultivar compared AR2017105, and at panicle initiation than at the tillering stage (Table 1).

3.2 | Estimation of AGB, PNU, and yield

Validation data showed that predictions of AGB, PNU, and yield were more accurate when imaging was conducted at the panicle initiation stage than at the tillering stage. The R^2 values for PNU, yield, and AGB varied from 0.72 to 0.75, 0.55 to 0.62, and 0.53 to 0.64, respectively, during the panicle initiation stage, while at the tillering stage, the values ranged from -0.07 to 0.23 for PNU, 0.18 to 0.43 for yield, and -0.08 to 0.24 for AGB (Table 2). The SVM had the highest accuracy for estimating AGB ($R^2 = 0.65$, RMSE = 1.70 Mg ha^{-1}, RMSPE = 19.4%), whereas MLR was the most effective model for yield estimation ($R^2 = 0.62$, RMSE = 1.18 Mg ha^{-1}, RMSPE = 21.8%). All models showed comparable accuracy in predicting PNU, with the highest R^2 value at 0.75 and the lowest RMSE and RMSPE at 88.69 kg N ha^{-1} and 23%, respectively (Figure 2; Table S5). Comparing the validation results with the calibration results, it appears that the model was not adequately validated for RF and ERT, suggesting an issue with overfitting (Table 2, Tables S5 and S6).

3.3 | Correlation analysis and feature importance

3.3.1 | Correlation between prediction features and response variables

At the rice tillering stage, both AGB and PNU showed very weak to weak correlations with individual bands, weak to moderate correlations with VIs, and moderate correlations with textural features (i.e., crop height and canopy) (Figure 3A). At the panicle initiation stage, AGB displayed

26396696, 2025, 1, Downloaded from https://acsess.onlinelibrary.wiley.com/doi/10.1002/agg2.70047 by CochraneAustria, Wiley Online Library on [14/02/2025]. See the Terms and Conditions (https://onlinelibrary.wiley.com/terms-and-conditions) on Wiley Online Library for rules of use; OA articles are governed by the applicable Creative Commons License

TABLE 2 Calibration and validation coefficients of determination (R^2) for the relationships between reflectance of unmanned aerial vehicle (UAV)-multispectral features and aboveground biomass (AGB, Mg ha^{-1}), plant nitrogen uptake (PNU, kg N ha^{-1}), and yield (Mg ha^{-1}), considering multiple linear regression (MLR), support vector machine (SVM), random forest (RF), and extremely random trees (ERT) models and Bands, VI, Bands + VI, Bands + VI + CHF input data.

		Calibration data						Validation data					
		Tillering stage (30 DAT)			Panicle initiation stage (60 DAT)			Tillering stage (30 DAT)			Panicle initiation stage (60 DAT)		
		R^2			R^2			R^2			R^2		
Model	Input data	AGB	PNU	Yield	AGB	PNU	Yield	AGB	PNU	Yield	AGB	PNU	Yield
MLR	Bands	0.30	0.34	0.54	0.68	0.75	0.66	0.14	0.15	0.4	0.64	0.72	0.61
	VI	0.30	0.33	0.53	0.68	0.77	0.66	0.14	0.15	0.39	0.63	0.74	0.62[a]
	Bands + VI	0.30	0.33	0.54	0.68	0.79	0.66	0.14	0.15	0.39	0.63	0.74	0.61
	Bands + VI + CHF	0.42	0.44	0.54	0.70	0.80	0.67	0.21	0.23	0.35	0.62	0.75	0.60
SVM	Bands	0.22	0.26	0.43	0.65	0.74	0.62	0.10	0.18	0.36	0.62	0.72	0.60
	VI	0.24	0.25	0.49	0.66	0.76	0.63	0.13	0.16	0.43[a]	0.64	0.74	0.61
	Bands + VI	0.23	0.25	0.49	0.66	0.78	0.63	0.09	0.15	0.41	0.63	0.75	0.61
	Bands + VI + CHF	0.35	0.30	0.50	0.68	0.79	0.64	0.24[a]	0.16	0.4	0.65[a]	0.75	0.60
RF	Bands	0.84	0.86	0.90	0.94	0.96	0.94	−0.08	−0.07	0.24	0.53	0.72	0.57
	VI	0.88	0.88	0.91	0.94	0.96	0.94	0.12	0.11	0.36	0.57	0.73	0.57
	Bands + VI	0.88	0.88	0.91	0.94	0.96	0.94	0.12	0.17	0.38	0.57	0.74	0.59
	Bands + VI + CHF	0.88	0.89	0.90	0.94	0.96	0.94	0.17	0.26[a]	0.31	0.57	0.74	0.60
ERT	Bands	1.00	1.00	1.00	1.00	1.00	1.00	−0.19	−0.13	0.18	0.54	0.73	0.56
	VI	1.00	1.00	1.00	1.00	1.00	1.00	0.14	0.18	0.32	0.56	0.75	0.55
	Bands + VI	1.00	1.00	1.00	1.00	1.00	1.00	0.14	0.19	0.37	0.56	0.74	0.57
	Bands + VI + CHF	1.00	1.00	1.00	1.00	1.00	1.00	0.17	0.23	0.32	0.58	0.75[a]	0.61

Abbreviations: Bands, spectral bands; CHF, canopy cover and height features; DAT, days after transplanting; VI, vegetation indices.

[a]Best model.

26396696, 2025, 1, Downloaded from https://acsess.onlinelibrary.wiley.com/doi/10.1002/agg2.70047 by CochraneAustria, Wiley Online Library on [14/02/2025]. See the Terms and Conditions (https://onlinelibrary.wiley.com/terms-and-conditions) on Wiley Online Library for rules of use; OA articles are governed by the applicable Creative Commons License

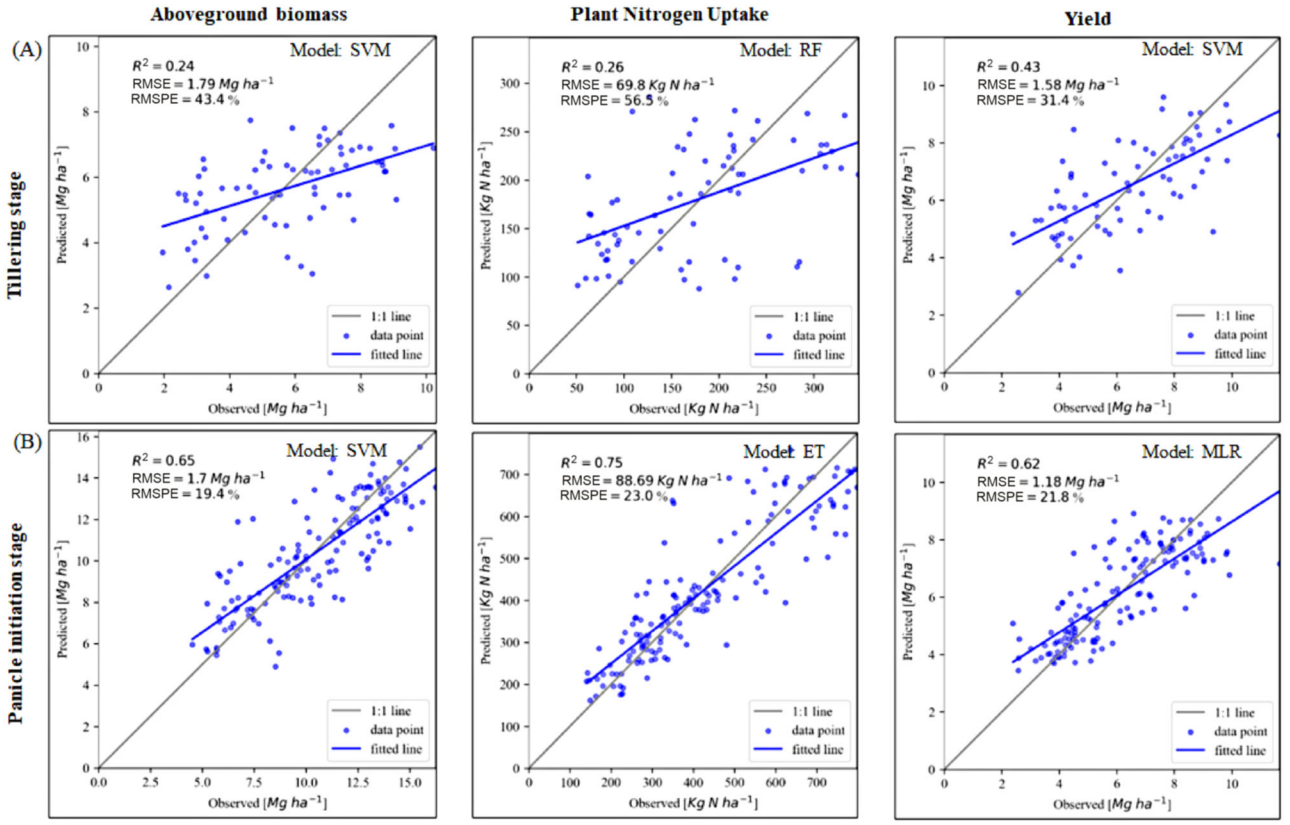

FIGURE 2 Relationships between predicted and observed aboveground biomass (AGB), plant nitrogen uptake (PNU), and yield of rice at the tillering (A, top row) and panicle initiation stages (B, bottom row), using the best model from Table 2. Model performance parameters are given. ET, extra trees; MLR, multiple linear regression; RF, random forest; RMSE, root mean square error; RMSPE, root mean square percentage error; SVM, support vector machine.

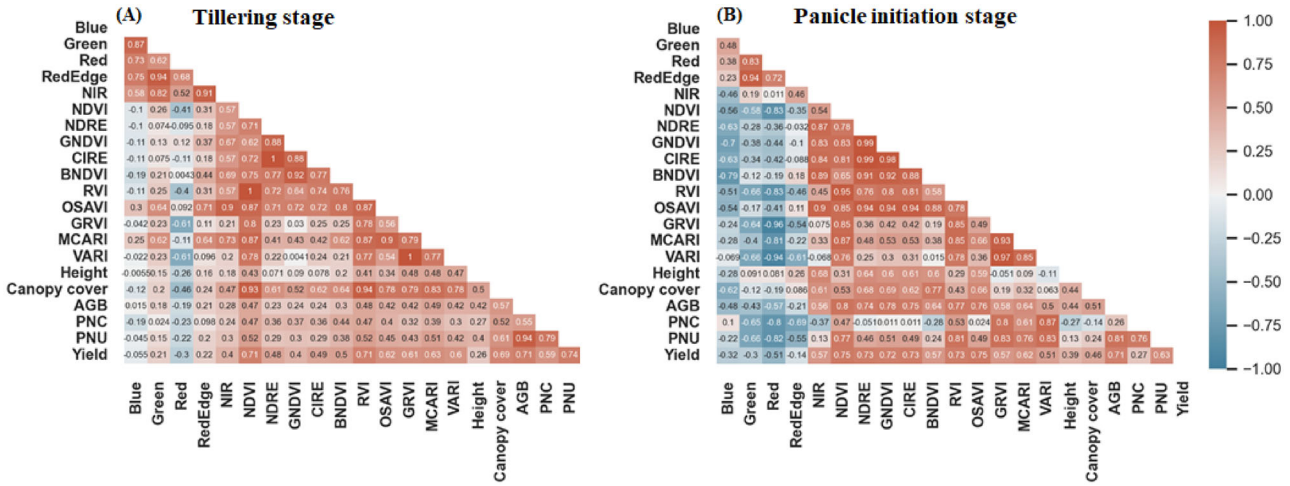

FIGURE 3 Correlation matrix of response variables and prediction features (see text and Table S4 for details on vegetation indices, incl. abbreviations) at the tillering stage (A) and panicle initiation stage (B); AGB, aboveground biomass; BNDVI, blue NDVI; CIRE, chlorophyll index-red-edge; GNDVI, green NDVI; GRVI, green red vegetation index; MCARI, modified chlorophyll absorption in reflective index; NDRE, normalized difference red-edge index; NDVI, normalized difference vegetation index; NIR, near infrared; RVI, ratio vegetation index; OSAVI, optimized soil adjusted vegetation index; PNC, plant nitrogen concentration; PNU, plant nitrogen uptake; RVI, ratio vegetation index; VARI, visible atmospherically resistant index.

26396696, 2025, 1, Downloaded from https://acsess.onlinelibrary.wiley.com/doi/10.1002/agg2.70047 by CochraneAustria, Wiley Online Library on [14/02/2025]. See the Terms and Conditions (https://onlinelibrary.wiley.com/terms-and-conditions) on Wiley Online Library for rules of use; OA articles are governed by the applicable Creative Commons License

strong correlations with most VIs, moderate correlations with textural features, and moderate but negative correlations with reflectance of most individual bands, except for the NIR band. PNU showed very weak to strong correlation with most single bands, moderate to very strong correlations with most VIs, and weak correlations with textural metrics (Figure 3B). Yield, at the tillering stage, displayed very weak to moderate correlations with single bands, moderate to strong correlations with VIs, and weak to strong correlations with textural features, whereas at panicle initiation stage, it showed strong correlations with most VIs, moderate correlations with textural metrics, and very weak to moderate negative correlations with single bands, except for the NIR band. Furthermore, the predictor variables show a high degree of multicollinearity (Figure 3).

3.3.2 | Feature importance

The results showed that VARI, RVI, and MCARI had the greatest impact on predicting PNU with importance scores of 41.2%, 25.9%, and 10.1%, respectively. For yield prediction, VARI, NIR band, MCARI, and RVI were the top four contributing features with importance scores of 27.3%, 20.6%, 19.1%, and 17.2%, respectively. For AGB prediction, important features included spectral information such as NIR band (22.1%), green band (15.9%), MCARI (15.1%), and VARI (12.3%), and crop height (13.4%) and canopy cover (11.1%) (Figure 4).

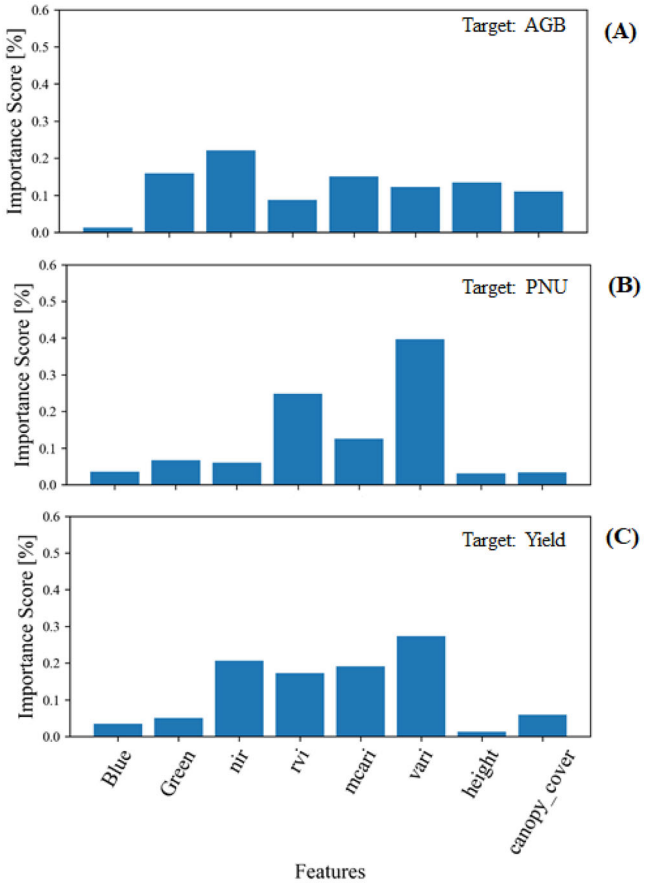

FIGURE 4 Feature importance at panicle initiation stage (days after transplanting [DAT] 60) for aboveground biomass (AGB) (A), plant nitrogen uptake (PNU) (B), and yield (C) of rice. MCARI, modified chlorophyll absorption in reflective index; NIR, near infrared; RVI, ratio vegetation index; VARI, visible atmospherically resistant index.

3.4 | Influence of management practices on paddy rice traits, VIs, and N uptake distribution maps

3.4.1 | Influence of management practices on paddy rice traits and VIs

The paddy rice traits consisted of the AGB, the PNU, and the yield, while the three spectral variables most sensitive to paddy rice N uptake (Figure 4), that is, VARI, RVI, and MCARI, were selected to assess their robustness in detecting agricultural management practices. The results showed that fertilization had a significant impact ($p < 0.05$) on the three indices and paddy rice traits at panicle initiation stage (Table 3). The VARI, RVI, and MCARI values were higher in plots where NPK was applied, either with or without BC, as opposed to areas where BC was applied alone or where no fertilizer was applied. Similar trends were observed for the paddy rice traits. However, no significant difference in index values was observed between cultivars and watering regimes (Table 3). Likewise, no significant differences in paddy rice traits were observed between cultivars and watering regimes, except for AGB, where TAI exhibited a greater AGB than AR2017105.

3.4.2 | N uptake distribution maps

The N uptake distribution maps in Kiringye (Figure 5) were generated based on the predicted PNU at the panicle initiation stage, using the ERT model, which had the highest accuracy (Figure 2). Most of the plots that received NPK (T3), NPK + BC (T4), and NPK + MCBC (T5) recorded the highest predicted PNU (Figure 5).

4 | DISCUSSION

4.1 | Paddy rice agronomic traits predictions

The best predictions were obtained at the panicle initiation stage when compared to the tillering stage for yield, AGB, and PNU (Table 2). Our results confirm previous studies that panicle initiation is the best time to collect rice canopy reflectance data (Harrell et al., 2011; Kanke et al., 2016; Stavrakoudis et al., 2019; Varinderpal-Singh et al., 2022). Measurements

26396696, 2025, 1, Downloaded from https://acsess.onlinelibrary.wiley.com/doi/10.1002/agg2.70047 by CochraneAustria, Wiley Online Library on [14/02/2025]. See the Terms and Conditions (https://onlinelibrary.wiley.com/terms-and-conditions) on Wiley Online Library for rules of use; OA articles are governed by the applicable Creative Commons License

TABLE 3 Paddy rice traits (aboveground biomass [AGB], plant nitrogen uptake [PNU], and yield) and vegetation indices (visible atmospherically resistant index [VARI], ratio vegetation index [RVI], and modified chlorophyll absorption in reflective index [MCARI]) as influenced by fertilization, cultivar, and watering regimes.

Factor		AGB	PNU	Yield	RVI	VARI	MCARI
Fertilizer type	Control	8.03 ± 0.45b	183.08 ± 10.49b	4.64 ± 0.24c	10.69 ± 0.47b	0.55 ± 0.01b	0.40 ± 0.02b
	BC	8.41 ± 0.46b	181.81 ± 11.73b	4.64 ± 0.24c	9.99 ± 0.28b	0.54 ± 0.01b	0.39 ± 0.02b
	MCBC	8.60 ± 0.44b	203.74 ± 16.00b	4.87 ± 0.18c	10.37 ± 0.47b	0.55 ± 0.01b	0.40 ± 0.02b
	NPK	12.13 ± 0.44a	322.16 ± 13.07a	7.02 ± 0.29b	18.53 ± 0.48a	0.67 ± 0.01a	0.51 ± 0.02a
	NPK + BC	12.88 ± 0.35a	358.91 ± 17.57a	7.81 ± 0.33ab	17.47 ± 0.81a	0.67 ± 0.01a	0.50 ± 0.02a
	NPK + MCBC	12.96 ± 0.37a	351.82 ± 16.35a	7.91 ± 0.28a	17.80 ± 0.55a	0.67 ± 0.01a	0.51 ± 0.02a
Cultivars	AR2017105	9.75 ± 0.47b	245.56 ± 15.57a	6.55 ± 0.28a	13.68 ± 0.63a	0.61 ± 0.01a	0.45 ± 0.01a
	TAI	11.25 ± 0.36a	288.27 ± 14.66a	5.75 ± 0.28a	14.60 ± 0.76a	0.61 ± 0.01a	0.45 ± 0.01a
Watering regimes	AWD	10.77 ± 0.46a	280.80 ± 16.67a	6.19 ± 0.27a	14.75 ± 0.70a	0.63 ± 0.01a	0.49 ± 0.01a
	PF	10.23 ± 0.41a	253.03 ± 13.94a	6.11 ± 0.30a	13.53 ± 0.69a	0.58 ± 0.01a	0.41 ± 0.01a

Note: Means ± SE in the same column and the same factor followed by different letters are statistically different (Tukey test, $p < 0.05$).
Abbreviations: AWD, alternate wetting and drying; BC, biochar; Control, unfertilized control, MCBC, manure-charged biochar; NPK + BC, mineral fertilizer + biochar; NPK + MCBC, mineral fertilizer + manure-charged biochar; NPK, mineral fertilizer; PF, permanent flooding.

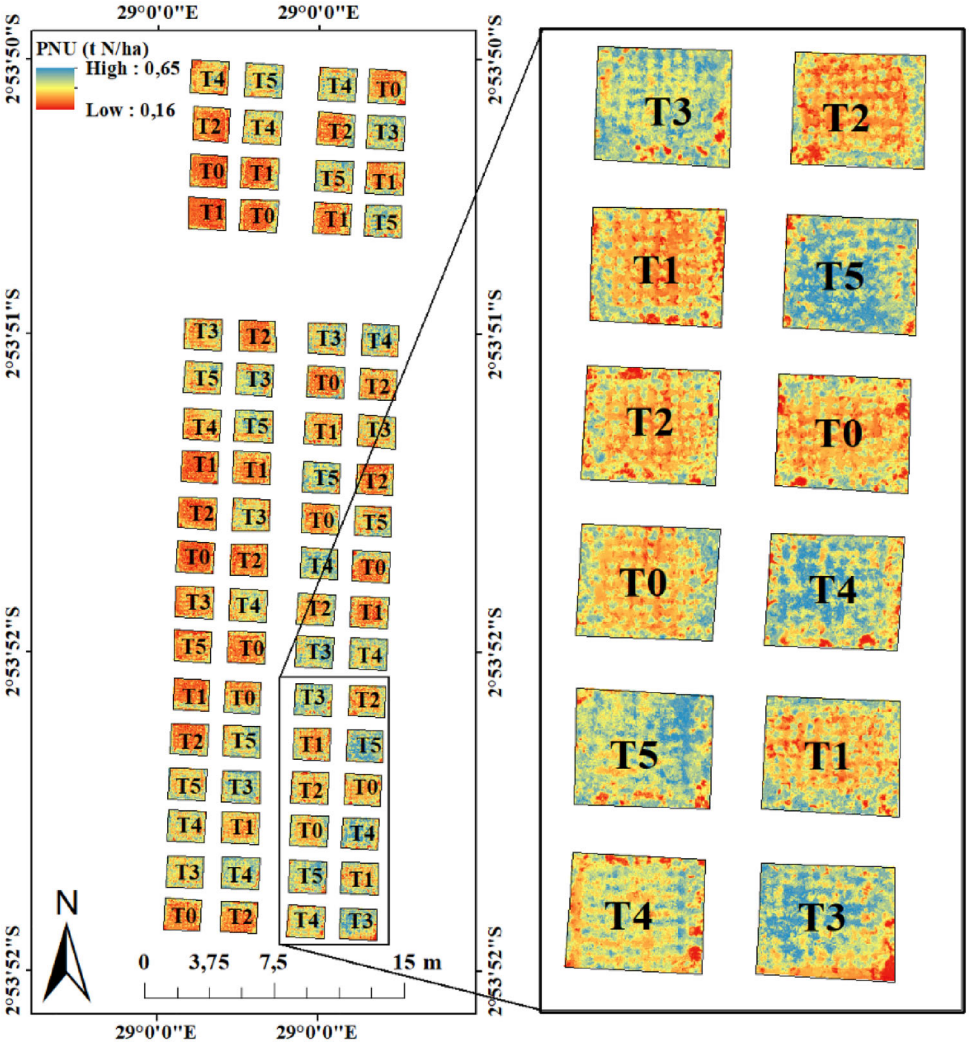

FIGURE 5 Plant nitrogen uptake (PNU) distribution within experimental plots in Kiringye, at panicle initiation stage (days after transplanting [DAT] 60); T0: unfertilized control, T1: rice husk biochar, T2: manure-charged biochar, T3: NPK, T4: NPK + BC, T5: NPK + MCBC; PF: permanent flooding, AWD: alternate wetting and drying.

26396696, 2025, 1, Downloaded from https://acsess.onlinelibrary.wiley.com/doi/10.1002/agg2.70047 by CochraneAustria, Wiley Online Library on [14/02/2025]. See the Terms and Conditions (https://onlinelibrary.wiley.com/terms-and-conditions) on Wiley Online Library for rules of use; OA articles are governed by the applicable Creative Commons License

taken before panicle initiation are often affected by water and soil in the background, while those taken after panicle initiation are either saturated or obscured by the emergence of panicles, which interferes with the spectral signal (Rehman et al., 2022).

The results also showed that the predictions of paddy rice traits in the Ruzizi plains were not greatly affected by the choice of model. Most studies using ML techniques for crop trait prediction report better performance of decision tree-based algorithms (i.e., RF or ERT) compared to linear-based algorithms (i.e., SVM or MLR) (Lussem et al., 2022; Yin et al., 2023; Zha et al., 2020). However, a strong generalization ability and comparable accuracy have been recognized for linear-based ML techniques such as SVM, especially when dealing with small databases or when training data are limited (Kok et al., 2021; Mountrakis et al., 2011), as is the case for this research. This may explain the relatively similar results obtained by the investigated models.

When comparing the three rice agronomic traits studied, higher prediction accuracy was obtained for PNU compared to AGB and yield (Table 2; Figure 2). A possible explanation for this is that UAV-spectral data were collected at 30 and 60 DAT, while harvest occurred around 120 DAT. This leaves nearly three-quarters to half of the growing season open to a variety of factors (biological, climatic, etc.) that can influence further development until harvest (Rehman et al., 2022). For example, in this study, local pests such as frogs and birds may have reduced some panicles or disrupted grain filling in some plants. This could potentially affect the predicted yields in the affected areas.

4.2 | Feature importance analysis

Spectral (NIR band, green band, VARI, and MCARI) and textural (plant height and canopy cover) features were both critical for predicting AGB, with spectral and textural data accounting for 65.4% and 24.5%, respectively (Figure 4). These findings are consistent with previous research showing that combining textural and spectral information improved the accuracy of rice biomass estimation compared to using spectral information alone (Cen et al., 2019; Maimaitijiang et al., 2019; Zheng et al., 2018). As plant N content is highly correlated with chlorophyll content, chlorophyll-sensitive VIs such as MCARI, RVI, and NIR and green bands are expected to improve the predictive capabilities of models for N-related traits like AGB and PNU (Stavrakoudis et al., 2019). In accordance, our analysis revealed that VARI, RVI, and MCARI contributed 76.8% to the prediction of PNU. Previous research has further shown that red-edge-based indices (e.g., MCARI), as well as NIR and red-edge reflectance, can effectively mitigate the effects of background noise and provide excellent predictive capabilities for chlorophyll content, thereby aiding in the accurate determination of N quantity (Colovic et al., 2022; Daughtry et al., 2000; Moreno-García et al., 2018). Dimyati et al. (2023) have also documented high correlation and similar effectiveness between the VARI, an RGB-based index, and NDVI in the monitoring the growth status and greenness of rice.

For yield prediction, VARI, MCARI, and RVI, as well as the NIR band, were the top four contributing features, with 84.2% contribution. These findings are in line with those of Zhou et al. (2017), who reported that VIs composed of reflectance within red-edge bands (e.g., MCARI in the case of this study) and NIR bands (e.g., RVI) were effective in predicting yield and biomass. This was also found by Perros et al. (2021) in a study on spatial analysis of agronomic data and UAV imagery for rice yield estimation. Zhou et al. (2017) further found that the features and indices that showed strong relationships with leaf area index and biomass (e.g., VARI in the case of this study) also performed well in yield prediction.

The results on feature importance confirm the importance of VIs composed of NIR and red-edge bands in the prediction traits and support the necessity to consider crop textural information, particularly when predicting rice AGB in the Ruzizi plains and similar cropping systems (Cen et al., 2019; Stavrakoudis et al., 2019). In addition, the VARI, an RGB-based VI can be highlighted as a convenient, available, and efficient indicator for monitoring rice paddy fields (Dimyati et al., 2023).

4.3 | VIs' ability in assessing in-season paddy rice management practices

To improve N management, farmers and other agricultural stakeholders need assessments of crop N status. This requires knowledge of the current N status of the crop and how likely it is to react to extra N applications (F. Li et al., 2010; Rehman et al., 2022). This study showed that VARI, MCARI, and RVI can detect paddy rice N uptake differences within heterogeneous field sites reflecting different management measures. Higher index values were recorded in areas where NPK, supplemented or not with BC, was applied, in contrast to areas treated with sole BC or where no fertilizer was applied. This is in line with previous studies reporting a significant and positive impact of N levels on NIR and red-edge-based indices (e.g., RVI and MCARI; [Colovic et al., 2022; Daughtry et al., 2000; Stavrakoudis et al., 2019; Y. P. Wang et al., 2022]). VARI was recently proposed by Dimyati et al. (2023) to be an effective VI for paddy rice monitoring as it can detect changes caused by biomass accumulation, is responsive to chlorophyll levels in leaves, and can therefore be correlated with PNU.

26396696, 2025, 1, Downloaded from https://acsess.onlinelibrary.wiley.com/doi/10.1002/agg2.70047 by CochraneAustria, Wiley Online Library on [14/02/2025]. See the Terms and Conditions (https://onlinelibrary.wiley.com/terms-and-conditions) on Wiley Online Library for rules of use; OA articles are governed by the applicable Creative Commons License

The results of our study showed that no significant differences in paddy rice traits and index values were obtained when comparing permanently flooded (PF) plots with alternate watering (AWD; Table 3). This indicates that the implementation of AWD irrigation did not induce any observable water-related stress in the plants, which could potentially affect the growth of paddy rice, alter its internal structure and canopy architecture, and subsequently affect its spectral reflectance properties (Y. P. Wang et al., 2022). AWD irrigation enables rice plants' roots to uptake water from the perched water in the root zone or the saturated soil, thereby preventing water stress (Bouman et al., 2007; Kumar & Rajitha, 2019). However, in the case of severe AWD, when water is allowed to drop below 15 cm from the soil surface, the plant can be exposed to water stress. Supporting this, Ramos-Fernández et al. (2024) used a UAV-based crop water stress index (CWSI) to compare AWD irrigation at a water level of 20 cm below the soil surface with traditional PF irrigation. They found that the CWSI values under AWD irrigation were higher.

TAI and AR2017105 are two important cultivars in the Ruzizi plain. TAI is one of the three commonly grown cultivar, while AR2017105 is being popularized since 2021 in different rice-producing areas of Ruzizi plain by the provincial Ministry of Agriculture (Bisimwa et al., 2019; IPA, 2022). Data collected by UAVs can be influenced by the cultivar due to a number of plant internal and architectural factors, including canopy size, shape, composition, and arrangement, which affect the interactions between incident radiation and plants (Ollinger, 2010). Therefore, to develop and apply uniform crop monitoring strategies in the Ruzizi plains, it is important that no significant differences in index values were obtained between the two investigated cultivars, despite their differences in AGB (Table 3). However, it remains necessary to determine, for a given species, whether and to what extent the cultivar influences optical sensor measurement (de Souza et al., 2020). Further studies expanding agricultural monitoring across the Ruzizi plains, covering ~800 km^2 of rice production area, thus need to gather detailed characteristics of the monitored cultivars and validate the models.

Overall, our results show that non-destructive measurements of paddy rice spectral reflectance between the visible and NIR bands can provide a rapid method for paddy rice monitoring during the growing season and for N management at rice production sites with different environmental properties and agronomic practices.

5 | CONCLUSIONS

This study employed two linear-based models and two decision tree-based models to predict paddy rice AGB, PNU, and yield using UAV multispectral images. The results showed that the phenological stage at which the UAV images were collected had a greater impact on the accuracy of the paddy rice traits prediction than the model selection. The panicle initiation stage recorded the most accurate predictions for yield, AGB, and PNU. Feature importance analysis revealed that VARI, MCARI, and RVI indices, along with NIR and green bands, played a critical role in predicting N uptake and yield in paddy rice. The same spectral features associated with crop height and canopy data were essential for predicting paddy rice AGB. It was also demonstrated that non-destructive measurements of paddy rice spectral reflectance between the visible and NIR bands can provide a rapid method for assessing crop trait variations caused by field management, with an emphasis on the VARI, an RGB-based index that could enable efficient and cost-effective monitoring. The UAV-based multispectral data can therefore provide valuable insights for making informed decisions on nutrient and water management techniques, and therefore they can be used by extension services to provide better management advice to farmers in order to close the rice yield gap in DRC. Further studies to scale up agricultural monitoring in the Ruzizi plains need to gather detailed characteristics on the majority of cultivars and include all two yearly cropping cycles and validate the models. Finally, the accuracy of the paddy rice trait predictions can be improved by integrating UAV-collected data and crop growth models that incorporate climate, soil, and other factors—requiring the establishment of fine-grid soil maps (incl. extension of flooding), the establishment of representative weather stations, and, for example, regular pest monitoring.

AUTHOR CONTRIBUTIONS

Daniel Muhindo: Conceptualization; data curation; formal analysis; funding acquisition; investigation; methodology; project administration; software; validation; visualization; writing—original draft; writing—review and editing. **Joyce J. Lelei**: Conceptualization; funding acquisition; methodology; supervision; validation; visualization; writing—original draft; writing—review and editing. **Wivine Munyahali**: Conceptualization; funding acquisition; methodology; project administration; supervision; validation; visualization; writing—review and editing. **Landry Cizungu**: Conceptualization; funding acquisition; methodology; project administration; supervision; validation; visualization; writing—review and editing. **Sebastian Doetterl**: Resources; validation; visualization; writing—review and editing. **Florian Wilken**: Resources; validation; visualization; writing—review and editing. **Espoir Bagula**: Validation; visualization; writing—review and editing. **Nathan Okole**: Data curation; formal analysis; methodology; validation; visualization; writing—review and editing. **Boris Rewald**: Conceptualization; funding acquisition; methodology; project administration; resources; supervision; validation;

26396696, 2025, 1, Downloaded from https://acsess.onlinelibrary.wiley.com/doi/10.1002/agg2.70047 by CochraneAustria, Wiley Online Library on [14/02/2025]. See the Terms and Conditions (https://onlinelibrary.wiley.com/terms-and-conditions) on Wiley Online Library for rules of use; OA articles are governed by the applicable Creative Commons License

visualization; writing—original draft; writing—review and editing. **Samuel Mwonga**: Conceptualization; funding acquisition; methodology; project administration; supervision; validation; visualization; writing—review and editing.

ACKNOWLEDGMENTS

We deeply appreciate the assistance provided during fieldwork by Henry Bisimwa, Fabien Munzihirwa, Benjamin Rwizibuka, Josué Matabaro, Fortunat Mpigirwa, Lionel Rhuhanga, Liliane Nabintu, Yvan Kika, and Yves Mugaruka, and for lab work by Marcel Hirsch, Leon Nabahungu, Dieudonné Chiragaga, and Rukiranuka Bienvenu. The research has been supported by the Austrian-African Research Network Africa-UniNet in the project "NuMaRice-UAV" and RUFORUM. Boris Rewald was supported by the EU Horizon project EXCELLENTIA (grant number 101087262) at Mendel University in Brno during the manuscript preparation phase.

CONFLICT OF INTEREST STATEMENT

The authors declare no conflicts of interest.

DATA AVAILABILITY STATEMENT

The datasets generated and analyzed during this study are available from the corresponding author upon request. All other data are included in this published article and its Supplementary Information files, and no third-party data have been used.

ORCID

Daniel Muhindo https://orcid.org/0000-0002-6964-1899
Boris Rewald https://orcid.org/0000-0001-8098-0616

REFERENCES

Adão, T., Hruška, J., Pádua, L., Bessa, J., Peres, E., Morais, R., & Sousa, J. J. (2017). Hyperspectral imaging: A review on UAV-based sensors, data processing and applications for agriculture and forestry. *Remote Sensing*, *9*(11), 1110. https://doi.org/10.3390/rs9111110

Balasubramanian, V., Sie, M., Hijmans, R. J., & Otsuka, K. (2007). Increasing rice production in sub-Saharan Africa: Challenges and opportunities. *Advances in Agronomy*, *94*(06), 55–133. https://doi.org/10.1016/S0065-2113(06)94002-4

Birindwa, R. D., Van Laere, J., Munyahali, W., De Bauw, P., Dercon, G., Kintche, K., & Merckx, R. (2023). Early planting of cassava enhanced the response of improved cultivars to potassium fertilization in South Kivu, Democratic Republic of Congo. *Field Crops Research*, *296*, 108903.

Bisimwa, B. E., Bagula, M. E., Birindwa, R. D., Byakombe, M., & et Mongane, E. (2019). *Rapport sur la sélection participative des variétés du riz dans la plaine de la Ruzizi, dans le cadre de la préparation du projet PICAGL.*

Bouman, B. A. M., Humphreys, E., Tuong, T. P., & Barker, R. (2007). Rice and water. *Advances in Agronomy*, *92*(04), 187–237. https://doi.org/10.1016/S0065-2113(04)92004-4

Brewer, K., Clulow, A., Sibanda, M., Gokool, S., Odindi, J., Mutanga, O., Naiken, V., Chimonyo, V. G. P., & Mabhaudhi, T. (2022). Estimation of maize foliar temperature and stomatal conductance as indicators of water stress based on optical and thermal imagery acquired using an unmanned aerial vehicle (UAV) platform. *Drones*, *6*(7), 169. https://doi.org/10.3390/drones6070169

Bulambo, K., Azadi, H., Polepole, S., Nabintu, M., Bembeleza, E., Dontsop, P., Masimane, J., Haurez, B., Fofana, M., & Lassois, L. (2023). Consumer preference for rice grain quality in the South Kivu and Tanganyika Provinces, eastern DR congo. *Foods*, *12*(21), 3995. https://doi.org/10.3390/foods12213995

Cen, H., Wan, L., Zhu, J., Li, Y., Li, X., Zhu, Y., Weng, H., Wu, W., Yin, W., Xu, C., Bao, Y., Feng, L., Shou, J., & He, Y. (2019). Dynamic monitoring of biomass of rice under different nitrogen treatments using a lightweight UAV with dual image-frame snapshot cameras. *Plant Methods*, *15*(1), 1–16. https://doi.org/10.1186/s13007-019-0418-8

Colovic, M., Yu, K., Todorovic, M., Cantore, V., Hamze, M., Albrizio, R., & Stellacci, A. M. (2022). Hyperspectral vegetation indices to assess water and nitrogen status of sweet maize crop. *Agronomy*, *12*(9), 1–17. https://doi.org/10.3390/agronomy12092181

Daughtry, C. S. T., Walthall, C. L., Kim, M. S., de Colstoun, E. B., & McMurtrey, J. E (2000). Estimating corn leaf chlorophyll concentration from leaf and canopy reflectance. *Remote Sensing of Environment*, *74*, 229–239. https://doi.org/10.1016/S0034-4257(00)00113-9

de Souza, R., Grasso, R., Peña-Fleitas, M. T., Gallardo, M., Thompson, R. B., & Padilla, F. M. (2020). Effect of cultivar on chlorophyll meter and canopy reflectance measurements in cucumber. *Sensors*, *20*(2), 509. https://doi.org/10.3390/s20020509

Dimyati, M., Supriatna, S., Nagasawa, R., Pamungkas, F. D., & Pramayuda, R. (2023). A comparison of several UAV-based multispectral imageries in monitoring rice paddy (a case study in paddy fields in Tottori prefecture, Japan). *ISPRS International Journal of Geo-Information*, *12*(2), 36. https://doi.org/10.3390/ijgi12020036

Espoir, M. B., Jackson, G. M. M., Gustave, N. M., Twaha, A. B., John, B. T., Sarah, A., Jean-Gomez, M. M., Geofrey, G., Patrick, M., Cephas, B. M., & Moses, M. T. (2021). Water and nutrient balances under selected soil and water conservation practices in semi-arid Ruzizi plain, Eastern Democratic Republic of Congo. *African Journal of Agricultural Research*, *17*(11), 1407–1419. https://doi.org/10.5897/ajar2021.15699

Geurts, P., Ernst, D., & Wehenkel, L. (2006). Extremely randomized trees. *Machine Learning*, *63*(1), 3–42. https://doi.org/10.1007/s10994-006-6226-1

Han, J., Zhang, Z., Cao, J., Luo, Y., Zhang, L., Li, Z., & Zhang, J. (2020). Prediction of winter wheat yield based on multi-source data and machine learning in China. *Remote Sensing*, *12*(2), 236. https://doi.org/10.3390/rs12020236

Hapfelmeier, A., & Ulm, K. (2013). A new variable selection approach using Random Forests. *Computational Statistics and Data Analysis*, *60*(1), 50–69. https://doi.org/10.1016/j.csda.2012.09.020

Harrell, D. L., Tubaña, B. S., Walker, T. W., & Phillips, S. B. (2011). Estimating rice grain yield potential using normalized difference vegetation index. *Agronomy Journal*, *103*(6), 1717–1723. https://doi.org/10.2134/agronj2011.0202

Hassler, S. C., & Baysal-Gurel, F. (2019). Unmanned aircraft system (UAS) technology and applications in agriculture. *Agronomy*, *9*(10), 618. https://doi.org/10.3390/agronomy9100618

26396696, 2025, 1, Downloaded from https://acsess.onlinelibrary.wiley.com/doi/10.1002/agg2.70047 by CochraneAustria, Wiley Online Library on [14/02/2025]. See the Terms and Conditions (https://onlinelibrary.wiley.com/terms-and-conditions) on Wiley Online Library for rules of use; OA articles are governed by the applicable Creative Commons License

IPA, I. de l'agriculture. (2021). *Rapport annuel de l'Inspection provinciale de l'agriculture. Bureau production et protection des végétaux (PPV)*.

IPA, I. de l'agriculture. (2022). *Rapport annuel de l'Inspection provinciale de l'agriculture. Bureau production et protection des végétaux (PPV)*.

IRRI. (2012). *Charactéristiques et description de la variété TAI*.

Kanke, Y., Tubaña, B., Dalen, M., & Harrell, D. (2016). Evaluation of red and red-edge reflectance-based vegetation indices for rice biomass and grain yield prediction models in paddy fields. *Precision Agriculture*, *17*(5), 507–530. https://doi.org/10.1007/s11119-016-9433-1

Kok, Z. H., Shariff, A. R. M., Alfatni, M. S. M., & Khairunniza-Bejo, S. (2021). Support vector machine in precision agriculture: A review. *Computers and Electronics in Agriculture*, *191*, 106546.

Kumar, K. A., & Rajitha, G. (2019). Alternate wetting and drying (AWD) irrigation—A smart water saving technology for rice : A review. *International Journal of Current Microbiology and Applied Sciences*, *8*(03), 2561–2571. https://doi.org/10.20546/ijcmas.2019.803.304

Li, F., Miao, Y., Hennig, S. D., Gnyp, M. L., Chen, X., Jia, L., & Bareth, G. (2010). Evaluating hyperspectral vegetation indices for estimating nitrogen concentration of winter wheat at different growth stages. *Precision Agriculture*, *11*(4), 335–357. https://doi.org/10.1007/s11119-010-9165-6

Li, X., Ba, Y., Zhang, M., Nong, M., Yang, C., & Zhang, S. (2022). Sugarcane nitrogen concentration and irrigation level prediction based on UAV multispectral imagery. *Sensors*, *22*(7), 2711. https://doi.org/10.3390/s22072711

Liu, S., Zhang, B., Yang, W., Chen, T., Zhang, H., Lin, Y., Tan, J., Li, X., Gao, Y., Yao, S., Lan, Y., & Zhang, L. (2023). Quantification of physiological parameters of rice varieties based on multi-spectral remote sensing and machine learning models. *Remote Sensing*, *15*(2), 453. https://doi.org/10.3390/rs15020453

Lussem, U., Bolten, A., Kleppert, I., Jasper, J., Gnyp, M. L., Schellberg, J., & Bareth, G. (2022). Herbage mass, N concentration, and N uptake of temperate grasslands can adequately be estimated from UAV-based image data using machine learning. *Remote Sensing*, *14*(13), 3066. https://doi.org/10.3390/rs14133066

MacCarthy, D. S., Darko, E., Nartey, E. K., Adiku, S. G. K., & Tettey, A. (2020). Integrating biochar and inorganic fertilizer improves productivity and profitability of irrigated rice in Ghana, West Africa. *Agronomy*, *10*(6), 1–23. https://doi.org/10.3390/agronomy10060904

Maimaitijiang, M., Sagan, V., Sidike, P., Maimaitiyiming, M., Hartling, S., Peterson, K. T., Maw, M. J. W., Shakoor, N., Mockler, T., & Fritschi, F. B. (2019). Vegetation index weighted canopy volume model (CVM VI) for soybean biomass estimation from unmanned aerial system-based RGB imagery. *ISPRS Journal of Photogrammetry and Remote Sensing*, *151*, 27–41. https://doi.org/10.1016/j.isprsjprs.2019.03.003

Mboyerwa, P. A., Kibret, K., Mtakwa, P., & Aschalew, A. (2022). Lowering nitrogen rates under the system of rice intensification enhanced rice productivity and nitrogen use efficiency in irrigated lowland rice. *Heliyon*, *8*(3), e09140. https://doi.org/10.1016/j.heliyon.2022.e09140

Moreno-García, B., Casterad, M. A., Guillén, M., & Quílez, D. (2018). Agronomic and economic potential of vegetation indices for rice N recommendations under organic and mineral fertilization in Mediterranean regions. *Remote Sensing*, *10*(12), 1908. https://doi.org/10.3390/rs10121908

Mote, K., & Velchala, P. R. (2021). Alternate wetting and drying irrigation technology in rice. *Indian Farming*, *70*(4), 06–09.

Mountrakis, G., Im, J., & Ogole, C. (2011). Support vector machines in remote sensing: A review. *ISPRS Journal of Photogrammetry and Remote Sensing*, *66*(3), 247–259. https://doi.org/10.1016/j.isprsjprs.2010.11.001

O'Brien, R. M. (2007). A caution regarding rules of thumb for variance inflation factors. *Quality and Quantity*, *41*(5), 673–690. https://doi.org/10.1007/s11135-006-9018-6

Oladele, S. O., Adeyemo, A. J., & Awodun, M. A. (2019). Influence of rice husk biochar and inorganic fertilizer on soil nutrients availability and rain-fed rice yield in two contrasting soils. *Geoderma*, *336*, 1–11. https://doi.org/10.1016/j.geoderma.2018.08.025

Ollinger, S. V. (2010). Sources of variability in canopy reflectance and the convergent properties of plants. *New Phytologist*, *189*(2), 375–394. https://doi.org/10.1111/j.1469-8137.2010.03536.x

Osco, L. P., Junior, J. M., Ramos, A. P. M., Furuya, D. E. G., Santana, D. C., Teodoro, L. P. R., Gonçalves, W. N., Baio, F. H. R., Pistori, H., Junior, C. A., da, S., & Teodoro, P. E. (2020). Leaf nitrogen concentration and plant height prediction for maize using UAV-based multispectral imagery and machine learning techniques. *Remote Sensing*, *12*(19), 1–17. https://doi.org/10.3390/rs12193237

Peng, X., Chen, D., Zhou, Z., Zhang, Z., Xu, C., Zha, Q., Wang, F., & Hu, X. (2022). Prediction of the nitrogen, phosphorus and potassium contents in grape leaves at different growth stages based on UAV multispectral remote sensing. *Remote Sensing*, *14*(11), 2659. https://doi.org/10.3390/rs14112659

Perros, N., Kalivas, D., & Giovos, R. (2021). Spatial analysis of agronomic data and uav imagery for rice yield estimation. *Agriculture*, *11*(9), 809. https://doi.org/10.3390/agriculture11090809

Qiu, J., Wu, Q., Ding, G., Xu, Y., & Feng, S. (2016). A survey of machine learning for big data processing. *Eurasip Journal on Advances in Signal Processing*, *2016*(1), 67. https://doi.org/10.1186/s13634-016-0355-x

Ramos-Fernández, L., Gonzales-Quiquia, M., Huanuqueño-Murillo, J., Tito-Quispe, D., Heros-Aguilar, E., Flores del Pino, L., & Torres-Rua, A. (2024). Water stress index and stomatal conductance under different irrigation regimes with thermal sensors in rice fields on the northern coast of Peru. *Remote Sensing*, *16*(5), 796. https://doi.org/10.3390/rs16050796

Rehman, T. H., Lundy, M. E., & Linquist, B. A. (2022). Comparative sensitivity of vegetation indices measured via proximal and aerial sensors for assessing N status and predicting grain yield in rice cropping systems. *Remote Sensing*, *14*(12), 1–18. https://doi.org/10.3390/rs14122770

Stavrakoudis, D., Katsantonis, D., Kadoglidou, K., Kalaitzidis, A., & Gitas, I. Z. (2019). Estimating rice agronomic traits using drone-collected multispectral imagery. *Remote Sensing*, *11*(5), 545. https://doi.org/10.3390/rs11050545

Suvi, W. T., Shimelis, H., & Laing, M. (2020). Farmers' perceptions, production constraints and variety preferences of rice in Tanzania. *Journal of Crop Improvement*, *35*(1), 1–18. https://doi.org/10.1080/15427528.2020.1795771

Uyanık, G. K., & Güler, N. (2013). A study on multiple linear regression analysis. *Procedia—Social and Behavioral Sciences*, *106*, 234–240. https://doi.org/10.1016/j.sbspro.2013.12.027

Vanwinckelen, G., & Blockeel, H. (2012). On estimating model accuracy with repeated cross-validation. In *BeneLearn 2012: Proceedings of*

26396696, 2025, 1, Downloaded from https://acsess.onlinelibrary.wiley.com/doi/10.1002/agg2.70047 by CochraneAustria, Wiley Online Library on [14/02/2025]. See the Terms and Conditions (https://onlinelibrary.wiley.com/terms-and-conditions) on Wiley Online Library for rules of use; OA articles are governed by the applicable Creative Commons License

the 21st Belgian-Dutch Conference on Machine Learning (pp. 39–44). https://lirias.kuleuven.be/handle/123456789/346385

Varinderpal-Singh, K., Kaur, R., Mehtab-Singh, Mohkam-Singh, Harpreet-Singh, & Bijay-Singh (2022). Prediction of grain yield and nitrogen uptake by basmati rice through in-season proximal sensing with a canopy reflectance sensor. *Precision Agriculture*, *23*(3), 733–747. https://doi.org/10.1007/s11119-021-09857-0

Vwima, S. N., & Rushigira, C. (2020). Problématique de l'intégration de l'agriculture du Sud-Kivu à la République Démocratique de Congo dans la Communauté Economique des Pays des Grands Lacs. *Reperes et Perspectives Economiques*, *4*, 18–40.

Walangululu, M. J., Yohali, S. D., Bisimwa, B. B., Nankafu, M. R., Buzera, K. L., Bashagaluke, B. J., & Bisimwa, B. E. (2012). Performance of introduced irrigated rice varieties in Ruzizi plain, South Kivu province, DR Congo. In *Proceedings of the Third RUFORUM Biennial Regional Conference* (pp. 1631–1636). RUFORUM. http://www.repository.ruforum.org/system/tdf/Walangululu%2CM.J.etal.pdf?file=1&type=node&id=32050&force=

Wang, L., Chen, S., Li, D., Wang, C., Jiang, H., Zheng, Q., & Peng, Z. (2021). Estimation of paddy rice nitrogen content and accumulation both at leaf and plant levels from UAV hyperspectral imagery. *Remote Sensing*, *13*(15), 1–21. https://doi.org/10.3390/rs13152956

Wang, Y. P., Chang, Y. C., & Shen, Y. (2022). Estimation of nitrogen status of paddy rice at vegetative phase using unmanned aerial vehicle based multispectral imagery. *Precision Agriculture*, *23*(1), 1–17. https://doi.org/10.1007/s11119-021-09823-w

Weiss, M., Jacob, F., & Duveiller, G. (2020). Remote sensing for agricultural applications: A meta-review. *Remote Sensing of Environment*, *236*, 111402. https://doi.org/10.1016/j.rse.2019.111402

Xu, X., Xu, S., Jin, L., & Song, E. (2011). Characteristic analysis of Otsu threshold and its applications. *Pattern Recognition Letters*, *32*(7), 956–961. https://doi.org/10.1016/j.patrec.2011.01.021

Yang, G., Liu, J., Zhao, C., Li, Z., Huang, Y., Yu, H., Xu, B., Yang, X., Zhu, D., Zhang, X., Zhang, R., Feng, H., Zhao, X., Li, Z., Li, H., & Yang, H. (2017). Unmanned aerial vehicle remote sensing for field-based crop phenotyping: Current status and perspectives. *Frontiers in Plant Science*, *8*, 1–26. https://doi.org/10.3389/fpls.2017.01111

Yin, H., Huang, W., Li, F., Yang, H., Li, Y., Hu, Y., & Yu, K. (2023). Multi-temporal UAV imaging-based mapping of chlorophyll content in potato crop. *PFG—Journal of Photogrammetry, Remote Sensing and Geoinformation Science*, *91*(2), 91–106. https://doi.org/10.1007/s41064-022-00218-8

Yu, K., Li, F., Gnyp, M. L., Miao, Y., Bareth, G., & Chen, X. (2013). Remotely detecting canopy nitrogen concentration and uptake of paddy rice in the Northeast China Plain. *ISPRS Journal of Photogrammetry and Remote Sensing*, *78*, 102–115. https://doi.org/10.1016/j.isprsjprs.2013.01.008

Zha, H., Lu, J., Li, Y., Miao, Y., Kusnierek, K., & Batchelor, W. D. (2021). In-season calibration of the CERES-Rice model using proximal active canopy sensing data for yield prediction. In *13th European Conference on Precision Agriculture* (p. 263). Wageningen Academic Publishers.

Zha, H., Miao, Y., Wang, T., Li, Y., Zhang, J., Sun, W., Feng, Z., & Kusnierek, K. (2020). Improving unmanned aerial vehicle remote sensing-based rice nitrogen nutrition index prediction with machine learning. *Remote Sensing*, *12*(2), 215. https://doi.org/10.3390/rs12020215

Zhao, J., Kumar, A., Banoth, B. N., Marathi, B., Rajalakshmi, P., Rewald, B., Ninomiya, S., & Guo, W. (2022). Deep-learning-based multispectral image reconstruction from single natural color rgb image—Enhancing UAV-based phenotyping. *Remote Sensing*, *14*(5), 1272. https://doi.org/10.3390/rs14051272

Zheng, H., Cheng, T., Li, D., Yao, X., Tian, Y., Cao, W., & Zhu, Y. (2018). Combining unmanned aerial vehicle (UAV)-based multispectral imagery and ground-based hyperspectral data for plant nitrogen concentration estimation in rice. *Frontiers in Plant Science*, *9*, 936. https://doi.org/10.3389/fpls.2018.00936

Zhou, X., Zheng, H. B., Xu, X. Q., He, J. Y., Ge, X. K., Yao, X., Cheng, T., Zhu, Y., Cao, W. X., & Tian, Y. C. (2017). Predicting grain yield in rice using multi-temporal vegetation indices from UAV-based multispectral and digital imagery. *ISPRS Journal of Photogrammetry and Remote Sensing*, *130*, 246–255. https://doi.org/10.1016/j.isprsjprs.2017.05.003

SUPPORTING INFORMATION

Additional supporting information can be found online in the Supporting Information section at the end of this article.

How to cite this article: Muhindo, D., Lelei, J. J., Munyahali, W., Cizungu, L., Doetterl, S., Wilken, F., Bagula, E., Okole, N., Rewald, B., & Mwonga, S. (2025). Paddy rice traits estimation under varying management strategies using UAV technology. *Agrosystems, Geosciences & Environment*, *8*, e70047. https://doi.org/10.1002/agg2.70047

26396696, 2025, 1, Downloaded from https://acsess.onlinelibrary.wiley.com/doi/10.1002/agg2.70047 by CochraneAustria, Wiley Online Library on [14/02/2025]. See the Terms and Conditions (https://onlinelibrary.wiley.com/terms-and-conditions) on Wiley Online Library for rules of use; OA articles are governed by the applicable Creative Commons License